Fracturing Fluid Characterization: State-of-the-Art Facility and Advanced Technology

Subhash Shah (subhash@ffcf.ou.edu; 405-325-1105)
Mahmoud Asadi (masadi@ffcf.ou.edu; 405-325-1113)
Fracturing Fluid Characterization Facility
Department of Petroleum & Geological Engineering
The University of Oklahoma
1103 Lexington Dr.
Norman, OK 73069

Introduction

The petroleum industry has used hydraulic fracturing technique to stimulate low and high permeability oil and gas reservoirs to enhance their potential recoveries. Nevertheless, the design and implementation of a scientifically and economically sound fracturing job, due to the lack of knowledge of rheological behavior of hydraulic fracturing fluids under field conditions, remains a challenge. Furthermore, as often the case, the current level of technical knowledge with research institutes, service companies, and operators does not translate to field applications. One of the principal reasons for this *technology gap*, is the lack of understanding of the rheological behavior of hydraulic fracturing fluids under field conditions, which primarily relates to the limitations in scaling down the field conditions to the laboratory. The Fracturing Fluid Characterization Facility (FFCF) project was therefore, proposed with the intent of providing the industry with a better understanding of the behavior of these fracturing fluids and their proppant transport characteristics under downhole fracture condition. At the FFCF, a fully operational High Pressure Simulator (HPS), as seen in Figure 1, constitutes a vertical, variable width, parallel plate flow apparatus and is capable of operating at elevated temperatures (up to 250^{o}F) and pressures (up to 1200 psi). The HPS simulates, to the maximum degree practical, all conditions experienced by a fracturing fluid from its formulation on the surface, its flow down the wellbore, through perforations, its injection into the fracture, and its leakage into the rock formation (Figure 1). Together with the onsite auxiliary equipment (Figure 2), such as Mixing and Pumping System, Pre-conditioning System, Data Acquisition System, and Rheology Measuring System (Figure 2), the HPS is the most advanced fracture simulator available to conduct research, mimicking field conditions, in the following areas:

- Rheology Characterization of Fracturing Fluids
- Proppant Transport Simulations
- Proppant Transport Measurements
- Perforation Pressure Loss
- Coiled Tubing Friction Loss
- Dynamic Fluid Loss
- Heat Transfer Characterizations of Polymer Solutions

Research sponsored by Gas Research Institute under contract 5091-211-2114 and the U.S. Department of Energy under contract DE-FC21-92MC29077

State-of-the-Art Facility & Advanced Technology

The FFCF Project. The FFCF was established as an experimental facility funded by Gas Research Institute (GRI), U.S. Department of Energy (DOE), and the University of Oklahoma (OU) to provide research and engineering services to the petroleum industry. The MTS systems Corporation, Halliburton Energy Services, and RE/SPEC, Inc. also worked in partnership with OU's Schools of Petroleum and Geological Engineering, Electrical Engineering, and Aerospace and Mechanical Engineering to design and build the facility. The FFCF was initiated in 1991, began operation in 1993, and is located in the University Research Park on the North Campus of the University of Oklahoma, Norman, Oklahoma.

The High Pressure Simulator. The development of a fracture simulator started with the design and construction of a prototype. Experience gained during the construction and operation of the prototype in 1993 suggested that budgetary constraints would not allow large-scale fracture simulator to be built based on the operating principles originally proposed. Consequently, the former prototype was re-designated as the High Pressure Simulator. The internal dimensions of the slot are 7 ft (2.13 m) high and 9.3 ft (2.84 m) long. Fluid enters and exits the slot through perforation manifolds representative of a wellbore. Slot width can be adjusted dynamically over a range of 0 to 1.25 in. by a system of 12 hydraulically actuated platens. Each platen is 28 in. by 28 in. and the platens are laid out in a 3 by 4 matrix to form one face of the simulated fracture. Each platen surface can be covered with a replaceable simulated rock facing (1 in. thick) having a desired permeability and texture. Behind each facing is a system of fluid collection channels which route fluid loss to a point outside the flow cell for measurement. The inlet and exit manifolds (2.75 in. in diameter) are equipped with 22 perforations whose configurations and sizes can be easily changed using a series of blank and sized inserts. Other unique features of the HPS include the vision system for flow visualization of proppant-laden fluids and Laser Doppler Velocimeters (LDV) for accurate rheological characterization of various fluids.

Approach

A number of research areas have been targeted and investigated to establish a foundation for obtaining reliable results in downhole conditions and to transfer findings to the industry. The performed research areas and their corresponding results are presented in the following sections.

Rheological Characterization of Borate-Crosslinked 35 lb/Mgal Guar and Hydroxypropyl Guar Gels

This section presents the results of pre-conditioned fluid rheology tests conducted with borate-crosslinked Guar and Hydroxypropyl Guar **(**HPG), using the HPS over a pH range of 9 to 11, subjected to varying levels of shear history and temperature. Even though the effect of pH and temperature on the borate ion concentration is relatively well understood, the characterization of the shear state of the gel at field conditions is still in its infancy[1,2,3]. Accordingly, the effects of polymer type, temperature, fluid pH, and shear history on the rheology of borate-crosslinked fluids are investigated. The presented results show dramatic effects of shear history on the

rheology of borate-crosslinked gels. Certain gel formulations corresponding to specific pH and temperature conditions were found to be shear history insensitive. Furthermore, these shear history insensitive formulations were also found to exhibit an optimum viscosity which was independent of temperature over the range of ambient temperature to 185°F.

Fluids Investigated

Fluids studied included borate-crosslinked 35 lb/Mgal Guar gel and borate-crosslinked 35 lb/Mgal HPG gel. The borate-crosslinked Guar and HPG gels are investigated in the pH range of 9 to 11. A 12% (wt.) solution of sodium tetra-borate (borax) is used as crosslinking agent. The effects of temperature on the rheology of borate-crosslinked gels are investigated by testing fluids in the temperature range from ambient conditions to 185^{o}F. The wellbore shear histories are simulated by subjecting fluids to the same shear intensity for various durations inside the coiled tubing. The temperature simulation within the fracture is achieved by flowing fluids through a double pipe heat exchanger at low fracture shear rates.

Procedure

For crosslinked fluid evaluation, the linear gel is first prepared (pH 6.9 to 7.0) and its pH is raised by adding various quantities of 25% (wt.) sodium hydroxide to obtain linear polymer solution with pH of 9, 10, and 11. The base gel is then pumped continuously in a single-pass mode at 60 gal/min through the coiled tubing, heat exchanger, HPS slot, and into a disposal tank. The coiled tubing is bypassed for the tests without shear history. The crosslinker is injected at a predetermined constant flow rate into the suction of the centrifugal pump. The HPS slot gap widths are varied to obtain various nominal shear rates. The boron concentration used is 45 ppm for the Guar based gels while for the HPG based gels is 135 ppm. For elevated temperature tests, the collected crosslinked fluid samples are allowed to cool down to room temperature prior to making pH measurements. In general, the final pH values are 0.3 to 0.5 lower than the initial values measured with the pH adjusted base gels.

Results and Discussion

Static pressure ports placed at selected locations in the slot are utilized to measure the pressure drop along the length of the slot. At periodic intervals throughout the experiment, the data acquisition system collects and records pressure drop, flow rate, temperature, and other pertinent data. The rheological characterization of the fluid is achieved by determining the apparent viscosity, μ_a, of the test fluid. First, the wall shear stress, τ_w, in the slot is calculated using the following equation,

$$\tau_w = \frac{6w\Delta P}{L} \quad \text{.....(1)}$$

Then, the nominal shear rate, $\dot{\gamma}$, in the slot is calculated based on the flow rate and the slot dimensions as,

$$\dot{\gamma} = \frac{1.925Q}{w^2 H} \quad \text{.....(2)}$$

Thus, for a given flow rate, a range of shear rates can be obtained by simply changing the gap width of the slot. For these shear rates, the apparent viscosity of the fluid is determined by,

$$\mu_a = \frac{47880\tau_w}{\dot{\gamma}} \quad \text{.....(3)}$$

Over the shear rate range considered, borate-crosslinked fluids formulated at a particular pH and temperature were found to display different rheological behavior depending on the shear history experienced by the fluid. This shear history dependency of borate-crosslinked fluids can be remedied to a large extent by selecting a fluid with a proper pH for a certain temperature application. However, the selection of a suitable pH for a particular temperature application has to be performed with care. The reason is that a shear history independent borate-crosslinked fluid at a certain pH and temperature may not have sufficient viscosity to carry the proppant down to the fracture. Therefore, in view of the above discussion, we define an 'optimum fluid' to be characterized by both, a shear history independent and maximum viscosity over a range of pH and temperatures considered.

Borate-Crosslinked 35 lb/Mgal Guar. The variation of the apparent viscosity with shear rate is studied for a borate-crosslinked 35 lb/Mgal Guar gel with pH 9 at ambient temperature. Various shear durations of 1, 3, and 5 minutes at a nominal shear rate of 1400 sec^{-1} are considered in this investigation. The apparent viscosity of the borate-crosslinked Guar gel is found to be approximately an order of magnitude larger than that of the linear polymer solution. In addition, the viscosity of the borate-crosslinked gel is found to be characterized by a shear thinning behavior independent of shear history. However, the shear history independent behavior of the borate-crosslinked 35 lb/Mgal Guar gel is completely lost at pH 10 and ambient conditions. At this pH value and ambient temperature, the borate-crosslinked Guar gel is found to be characterized by a shear thinning, shear history dependent behavior with the viscosities obtained for no shear history much higher than those observed with shear history. A possible explanation for this interesting behavior is that the crosslinked bonds that are broken during the shearing action do not have enough time to reheal at this particular pH and temperature.

An increase in temperature to about 120°F shows that the shear history independent rheological behavior of the borate-crosslinked 35 lb/Mgal Guar gel with pH 9 is preserved. In addition, the apparent viscosities of the gels are found to be approximately the same for shear rates ranging from 20 to 200 sec^{-1}. The crosslinked gel is shown to be characterized by a more complex, shear history dependent rheological behavior.

Figure 3 shows the apparent viscosities for borate-crosslinked Guar gel with pH 9 at 150^0F. The apparent viscosities exhibit both shear thickening (at lower shear rates) as well as shear thinning (at higher shear rates) characteristics separated by a maxima at various shear histories. It is observed that the location of this inflection point in the apparent viscosity curve depends on the fluid pH, temperature, and shear rate, and to some extent, may even depend on the shear history of the crosslinked test fluid, Figure 3. An increase in the pH value to 10 for the borate-crosslinked Guar gel at the same temperature (150°F) revealed a shear thinning, shear history independent rheological behavior. As the pH value of the borate-crosslinked gel is

increased to 11, the apparent viscosities are seen to drop from the maximum value at pH 10. Since pH 11 did not yield a shear history independent fluid at 150°F, another test was conducted at a much higher temperature of 185°F. The results showed a shear history independent rheological behavior of the borate-crosslinked 35 lb/Mgal Guar gel at 185°F with an initial pH 11. A clear illustration of all of these above results is provided in the form of a bar chart in Figure 4. This figure indicates that there is an optimum viscosity at each temperature corresponding to a specific pH value. These pH values are seen to increase monotonically from 9 to 11 over the temperature range from ambient to 185°F. This figure also shows that the optimum viscosity values are essentially independent of temperature over this range

Borate-Crosslinked 35 lb/Mgal HPG. The apparent viscosity variation with shear rates ranging from 20 to 200 sec^{-1} are considered for a borate-crosslinked 35 lb/Mgal HPG gel for various shear histories, pH values and temperatures. The crosslinked HPG gel is characterized by a shear thinning, shear history independent behavior at ambient conditions. The effect of shear history is found to be more pronounced in the first minute of shear through the coiled tubing. In addition, the borate-crosslinked HPG gel is found to exhibit the same, complex rheological behavior characterized by both a shear thickening and shear thinning part at higher temperatures (150°F). Also, the 150^0F results show that as the pH is increased (pH 11), the borate-crosslinked 35 lb/Mgal HPG gel becomes shear history dependent. In comparison, the results show that both the borate-crosslinked 35 lb/Mgal Guar and HPG gels are found to exhibit similar rheological behavior with pH and temperature for all the shear rates and shear histories considered.

Development of Perforation Pressure Loss Correlations for Limited Entry Fracturing Treatment

Currently, the industry is using a sharp-edged orifice equation to estimate the pressure drop across a perforation[4]. This equation includes a kinetic energy correction factor commonly known as the "coefficient of discharge" and is in the form of,

$$\Delta P_{perf} = \frac{0.2369\mathrm{r}}{d^4 C_d^2}\left(\frac{Q}{N}\right)^2 \quad \text{.....(4)}$$

Although the coefficient of discharge depends on fluid type and orifice size, it is common practice to assume a fixed value for all fluids and perforation sizes. However, recent studies have shown that the coefficient of discharge can vary significantly with fluid viscosity and perforation size. Accordingly, investigation of the perforation pressure loss has been conducted for linear polymer solutions, crosslinked gels, and fracturing slurries. New correlations are developed to estimate the coefficient of discharge used in the orifice equation. The correlations can be used to accurately predict the coefficient of discharge for linear polymer solutions and titanium/borate-crosslinked gels. In addition, the slurry correlation can be utilized to determine the dynamic change in the coefficient of discharge for fracturing slurries due to erosion.

Procedure

Linear Polymer Solution. Linear polymer solution, approximately 1000 gallons of fresh linear polymer solution are prepared and circulated through the HPS using stainless steel perforations

sizes of 0.25″, 0.375″, and 0.5″. The perforation pressure loss data are obtained at different flow rates using two differential pressure transducers.

Crosslinked Gels. In a second test, approximately 100 bbls of fresh linear polymer solution is prepared in a mixing tank and then fed to the triplex pump using the centrifugal pump. The clean fluid is circulated through the HPS until a steady flow rate of 60 gpm is attained. As directing the base gel in a single pass, the crosslinker is added to the suction of the centrifugal pump at a rate of 1.5% (wt.) for HPG and 0.5% (wt.) for Guar. The discharge rate of the triplex pump is maintained at 60 gpm, and the fluid is pumped through the HPS using stainless steel perforation sizes of 0.25″, 0.375″, and 0.5″. Perforation pressure loss data are acquired at various flow rates so that the differential pressure across perforations remains less than 500 psi. Variable flow rates through the slot are attained by bypassing flow around the HPS while maintaining the discharge rate of the triplex pump constant. By following this procedure, the crosslinking rate is kept constant and uniform rheological properties for the crosslinked fluid are achieved.

To investigate the effect of shear history, discharge of the triplex pump is diverted through the full length of a 5000 ft coiled tubing at a flow rate of 60 gpm where the test fluid is subjected to shear for 5 minutes at 1400 sec^{-1}. Perforation pressure loss data are then obtained at various flow rates so that the differential pressure across perforations remain less than 100 psi. Variable flow rates through the slot are attained by bypassing flow around the HPS while maintaining the discharge rate of the triplex pump constant.

To investigate the effect of perforation size, proppant concentration, and sand size on perforation pressure loss, approximately 200 gallons of linear polymer solution are mixed with 20/40 mesh sand to prepare slurries with 0 to10 ppg sand concentrations. Four perforations of the same size (0.375″ or 0.5″), are installed at 8″ spacing. The differential pressure across the perforations is measured at different flow rates. The same procedure is followed with slurries prepared by mixing linear polymer solution with 12/20 mesh sand. The flow rates in these tests are kept low to avoid erosion effects. The sand slurries are prepared in the mixing tank with the desired concentration and pumped through the HPS at 3 bbl/min. Two steel-cement composite perforations of size 0.375″ with 16″ spacing is used and the pressure drop is measured.

Results and Discussion

Clean Fluids. A new coefficient of discharge based on the statistical analysis is developed for both linear HPG and titanium-crosslinked HPG as follows,

$$C_d = \left(1 - e^{\frac{-2.2d}{m_b^{0.1}}}\right)^{0.4}, \quad r^2 = 0.886 \quad \text{(for linear HPG)} \qquad (5)$$

$$C_d = \left(1 - e^{\frac{-1.76}{(m_b \cdot d)^{0.25}}}\right)^{0.6}, \quad r^2 = 0.962 \quad \text{(for titanium-crosslinked HPG)} \qquad (6)$$

Equations 5 and 6 can be used in conjunction with Eq. 4 to calculate the pressure loss across a perforation. Note that Eq. 5 predicts a coefficient of discharge of unity as perforation diameter is increased to ∞ and as the viscosity of the fluid approaches zero. Also, the coefficient

of discharge becomes zero when perforation diameter is zero and the fluid is extremely viscous (μ_a reaches infinity). Equation 6; however, does not meet this physical limitation. The predicted coefficient of discharge approaches unity as the perforation size becomes zero, which does not represent an actual physical limitation. The applicability of this correlation to other linear polymer solutions is verified against the experimental data obtained with 35 lb/Mgal Guar gum, Figure 5.

Sand Slurries. The coefficient of discharge for sand slurries is affected by various parameters in addition to the slurry viscosity and perforation diameter. The experiments have shown that with increased sand concentration, the perforation pressure loss increases while the coefficient of discharge decreases. This behavior becomes less significant as sand size increases. Moreover, the perforation pressure loss for 20/40 mesh sand slurries is higher than that of the 12/20 mesh sand slurries. This difference in perforation pressure loss between the two sand size slurries is due to the fact that 12/20 mesh sand slurry is less viscous than 20/40 mesh sand slurry for the same sand concentration.

Figure 6 presents the coefficient of discharge versus the total cumulative mass of sand pumped through the perforations at two different pump rates. The coefficient of discharge increases with increase in the total cumulative mass of sand pumped. However, at both pump rates the major change in the coefficient of discharge occurs during the early stages of slurry pumping and less dramatic change is experienced through the remainder of the time. Also, the coefficient of discharge tends to increase as pump rate increases. This implies that the dynamic change in the coefficient of discharge due to erosion is a function of the flow rate as well as the total cumulative mass of the sand pumped. Since the kinetic energy of the slurry is a function of slurry density, the coefficient of discharge is expected to change as sand concentration varies. To accurately estimate perforation pressure loss of fracturing slurries, the change in the coefficient of discharge has to be determined as a function of flow rate, sand concentration, and cumulative mass of sand pumped. Using the data obtained for a 20/40 mesh sand slurry and the dimensional analysis , the following correlation is developed:

$$C_d = \left\{ \left(1 - e^{\frac{-2.2d}{\mu_a^{0.1}}} \right)^{0.8} + A\Pi_3^{B} \right\}^{\frac{1}{2}} \quad \text{.....(7)}$$

where,

$$A = \frac{13.34\left(\Pi_2\right)^{5.48} e^{-8.7\Pi_2}}{13.20\left(\Pi_2\right)^{5.48} + 38\times 10^{-5}}$$

$$B = 0.4 - 993\left(0.5 - \Pi_2\right)^{3.82} e^{-12.6\left(0.5-\Pi_2\right)}$$

$$\Pi_2 = \frac{\Delta r\, Q}{\mu_a d} \le 0.5$$

$$\Pi_3 = \frac{\rho\, Q^2 t}{\mu_a d^4}$$

Figure 7 is the plot of the coefficient of discharge calculated using the perforation pressure loss data obtained from the erosion tests with 20/40 mesh sand slurry vs. the cumulative mass of the sand pumped. Also, research was performed on the effect of sand concentration on perforation erosion. The result predicts a higher erosion rate at intermediate sand concentrations. This is due to the fact that a lower sand concentration slurry has less kinetic energy than an intermediate sand concentration slurry. A higher sand concentration slurry, on the other hand, dissipates most of its kinetic energy due to sand particles friction. Therefore, it possesses less kinetic energy than the intermediate sand concentration slurry. Thus, for limited-entry treatments, this correlation can be used during the design stage to select the sand concentration that would produce minimum erosion.

Dynamic Fluid Loss

The shape and extension of the created fracture and whether the treatment will screen-out early or be pumped to completion depend on an accurate knowledge of fluid loss[6]. The fluid loss is usually a linear function of the square-root-of-time. It has been noted in the past by other investigators that the fluid loss is not always a linear function of the square-root-of-time, but may become a linear function of time[7]. The spurt loss is also an important parameter and is considered part of the fluid loss function. It is the initial loss of fluid to the formation as fresh formation comes in contact with the fracturing fluid. If the spurt loss is estimated too low, the treatment may screen-out early while high spurt loss estimates will underpredict the created fracture. Accordingly, field scaled dynamic fluid loss tests were performed on the HPS using permeable synthetic and natural rock facings, both linear polymer solutions and crosslinked gels, and with and without fluid loss additives.

Procedure

Permeable facings are mounted in the middle position on either side of the HPS slot. Each facing was initially permed with water at back-pressures ranging from 200 to 1000 psi. During the water permeability tests, a stabilized flow through the facing was determined using a graduated cylinder and stop watch. Following the water permeability tests, a dynamic fluid loss experiment was performed at 50 sec^{-1} shear rate and 1000 psi back-pressure using a specially designed throttling valve.

Results and Discussion

Synthetic Rock. Initially, a permeable synthetic (0.0522, 0.366, and 0.653 md) rock facings were developed to utilize the HPS in fluid loss tests using 60 lb/Mgal HPG without fluid loss additive. With no fluid loss control, the linear fluid flowed through the facing relatively unimpeded. Therefore, a 50 lb/Mgal silica flour was added to the solution to control fluid loss. The spurt loss and fluid loss coefficient were determined form the data gathered.

The results showed that the smooth surfaces of the synthetic facings did not develop filter cake while the natural rock facings developed a filter cake. Surface roughness was found to be the major factor in filter cake development. Linear gels left a moderate concentration of polymer in the filter cake formed when the synthetic facings were roughened by sand blasting and crosslinked gels left a much higher concentration of polymer. This period of development of fluid

loss testing in the HPS led to the study of the synthetic facings. The back half of the facing had about twice the porosity of the front half of the facing, but the permeability was consistent throughout. In the back half, the vast majority of pore throats ranged from 5 to 7 microns with an insignificant percentage of larger pores. The front half, however, had 12 to 15 % of the pore throats of 8.6 microns or larger. It is notable that, while the base gels with no fluid loss additive flowed through these facings relatively unimpeded, the addition of fluid loss additive or even crosslinker was sufficient to bring this fluid loss under control. These results indicate that no significant increase in fluid loss control was achieved by going from 25 lb/Mgal silica flour to 50 lb/Mgal. Also, it is concluded that crosslinker alone provides decent fluid loss control in this permeability range. The spurt loss for the 60 lb/Mgal test is about half of the spurt loss during the 40 lb/Mgal. Increasing the gel concentration for crosslinked fluids greatly enhances its fluid loss control characteristics. Results show a trend of increasing fluid loss with increasing permeability. Figures 8 and 9 show the behavior of borate crosslinked 35 lb/Mgal HPG without and with 25 lb/Mgal silica flour on medium permeability synthetic rock facings. A departure from linear with respect to square-root-of-time behavior is noted for borate crosslinked 35 lb/Mgal HPG. The permeability and the fluid loss coefficient, $C_{w,}$ differences are similar, however, the spurt loss for the gel with silica flour was about 1.5 times that of the gel without silica flour. For these tests, the surface of the synthetic rock facing was sandblasted to roughen it to produce filter cake.

Natural Rock. The results of a test conducted with titanium crosslinked 60 lb/Mgal HPG with 50 lb/Mgal silica flour, a 0.5" gap width, and 30 sec^{-1} shear rate using natural rock showed a slight departure from square-root-of-time behavior is developed at 37 minutes. The permeability for the natural rock facing is approximately 3 times that of the synthetic facing. The C_w for the natural rock test is almost 8 times that of the synthetic rock and the spurt loss is about half.

Natural Fracture Studies. Hydraulic pressure was applied to the back of the facing until the facing was fractured. A test with 40 lb/Mgal HPG produced a 7 gpm fluid loss when only the linear fluid was flowing through the fracture at 500 psi back pressure. When titanium crosslinked fluid entered the HPS, the fluid loss was reduced to 5 gpm. The test was concluded when a 0.5 lb/gal concentration of a 50:50 mixture of silica flour and 100 mesh sand in the linear fluid entered the slot. A total shutoff of fluid loss occurred. The titanium crosslinked 60 lb/Mgal fluid showed a steady decrease in fluid loss during the test, and a step decrease when the silica flour entered the slot. The borate crosslinked test was conducted on a naturally fractured Berea sandstone. Crosslinker addition and 25 lb/Mgal silica flour showed no great reductions in fluid loss rate. The late addition of 50 lb/Mgal silica flour showed a notable reduction in fluid loss. The total shutoff did not occur in this case and a filter cake was found on the facing upon conclusion of the test.

Control Mechanisms. Another aspect of fluid loss is its control mechanisms. Filter cake development on the surface of the fracture face was once thought to be the major factor in controlling fluid loss and filter cake developing fluids were designed. However, the use of synthesized rock for fluid loss studies at the FFCF has shown that external filter cake development is not a determining factor in fluid loss control. The use of the smooth faced synthesized rock slabs showed no or very little filter cake development in the HPS. Nevertheless, fluid loss control was achieved before this filter cake was developed. Studies were also performed on intentionally broken facings to simulate natural fractures. It was found that only high concentrations of properly sized solids were able to provide decent fluid loss control.

Tubular Friction Loss

A series of experiments were performed to estimate the frictional pressure losses that occur in coiled tubings during hydraulic fracturing treatment. The effects of curvature and seam on the frictional pressure losses in coiled tubing are reported for the fluids such as water, linear Guar gum and HPG, and borate-crosslinked gels. In addition, the effects of fluid pH and shear history on the frictional pressure losses are investigated. The results obtained with water indicate that the curvature as well as the seam inside the coiled tubing significantly affects the frictional pressure losses. However, the results obtained with various linear polymer solutions and crosslinked gels suggest that tubing curvature has a more significant effect on the frictional pressure losses than the tubing seam. Moreover the frictional pressure losses are found to be dependent on the fluid pH for both linear polymer solutions and crosslinked gels. Further, the frictional losses are found to be dependent on the shear history for borate-crosslinked HPG gel and independent of shear history for borate-crosslinked Guar gel.

Results and Discussion

To facilitate comparison of the experimental data with the theory for Newtonian fluids, experiments are first conducted with water as the test fluid. The straight sections of seamed (ID=1.1752 in.) and seamless tubing (ID=1.1817 in.) are considered and Reynolds numbers ranging from 1.3×10^5 to 3.2×10^5 (turbulent flow) are chosen for the analysis. The friction factors obtained for water in both seamed and seamless tubings are found to agree reasonably well with the corresponding friction factor values computed for the smooth pipe. In particular, the excellent agreement of the frictional factors obtained for the seamed tubing with the theory, may be attributed to the presence of the seam which tends to alter the turbulence spectrum by damping the high turbulence frequencies and thus, causing a decrease in the turbulent frictional pressure drop. A similar investigation performed with water in coiled tubing showed that the curvature of the coiled tubing has a significant effect on the frictional pressure loss and the friction factors obtained are in general much higher than those obtained in the straight sections of seamed and seamless tubing. For water, the friction factors for the straight sections of seamed and seamless tubing are found to be related by the following expression,

$$f_{seamed} = 1.667\left(N_{\mathrm{Re}}^{-0.049}\right) f_{seamless} \quad \text{.....(8)}$$

Where f_{seamed} is the friction factor for the straight seamed tubing and f_{seamless} is the friction factor for the straight seamless tubing. Similarly, the friction factors taking into account the effect of curvature of the pipe is related to the friction factors of the straight section of the seamed pipe by the following correlation,

$$f_{CT} = 0.6\left(N_{\mathrm{Re}}^{0.068}\right) f_{seamed} \quad \text{.....(9)}$$

The friction factor of coiled tubing is related to the corresponding friction factors of the straight sections of the seamless tubing by the following expression,

$$f_{CT} = 1.017\left(N_{\mathrm{Re}}^{\ 0.019}\right) f_{seamless} \quad \text{.....(10)}$$

The study also shows that the friction factor values obtained for a linear 0.4% Guar polymer solution (n=0.53, K=0.0112 psf sec^n) for the Reynolds number range of $2.0\text{x}10^3$ to $3.36\text{x}10^4$ (turbulent flow), are much lower than those obtained for water. In the range of Reynolds number considered, drag reduction varying from 29% to 78% is obtained with the polymer solution. Also, it is observed that the friction factor values determined for the coiled tubing are higher than those obtained for the straight sections. Nevertheless, tubing seam does not seem to have any effect on the friction factor. Since the seam tends to suppress the high turbulence frequencies, the results suggest that for the drag-reducing fluid under investigation, the turbulence spectrum is composed mainly of low-turbulence frequencies, on which the tubing seam has no effect. Examination of the experimental data suggest that coiled tubing friction factor, f_{CT}, is related to straight pipe friction factor, f_{SP} , by the following relationship,

$$f_{CT} = 0.747\left(N_{\mathrm{Re}_G}^{0.105}\right) f_{SP} \quad \text{.....(11)}$$

Where, N_{Re_G} is the generalized Reynolds number. The pressure drop results obtained for borate-crosslinked 35 lb Guar/Mgal polymer gel from measurements performed on straight seamed and seamless tubing sections is shown in Figures 10. The same study for pH 10 and 11 shows that the effect of shear history strongly depends on the fluid pH. For pH 9 fluid, the pressure drop decreases continuously with increasing shear history, while for pH 10 and 11 fluids, the frictional pressure drop first decreases to a minimum value corresponding to a shear history of one minute, then starts increasing with increasing shear history. This is explained by different mechanisms that are present as the fluid flows, namely, breaking of the crosslink bonds due to shearing, formation of new bonds, and rehealing of some of the broken bonds.

Heat Transfer

Fracturing fluids undergo considerable temperature and shear history variations while pumping down the wellbore. These temperature variations naturally affect the rheological properties of fracturing fluids. Therefore, to accurately characterize a fluid and improve fracture treatment design, the heat transfer characteristics of the fluids is investigated. To accurately quantify these properties and their effects on rheology, it is necessary to evaluate the heat transfer coefficients of fracturing fluids in a double pipe heat exchanger.

The heat transfer characteristics of fluids flowing in a heat exchanger mainly depends on the inlet and outlet temperatures of the hot and cold fluids. This difference provides a measure for the amount of heat lost by the hot fluid and the amount of heat gained by the cold fluid. The amount of heat transferred depends on the flow regime of the fluid, the temperature difference between the fluids, the amount of scale deposited on the tube walls, the thermal conductivity of the wall boundary separating them, and the specific heat of the fluids. Mathematically, the amount of heat transferred in the double pipe heat exchanger is represented by an overall heat transfer coefficient, *U*, given by,

$$U = \frac{60 Q_V \rho C_P \Delta T}{\Delta T_L A} \quad \text{.....(12)}$$

where:

$$\Delta T_L = \frac{\Delta T_1 - \Delta T_2}{\ln(\Delta T_1 / \Delta T_2)} \quad \text{.....(13)}$$

Procedure

The experiments were conducted on linear and borate crosslinked Guar, linear and borate crosslinked HPG, an 8 ppg sand slurry, and water. The crosslinker is batch mixed with linear Guar, linear and borate-crosslinked HPG, and an 8 ppg sand slurry for preparation of the test fluid and an activator is added on the fly. The fluid is preheated inside a heat exchanger to 150^{o}F by means of a hot oil unit with water as the heating medium. The flow rates are maintained at 60 gpm on the tube side and 40 gpm on the shell side in a crossflow arrangement. The temperature data is collected in three different sections of the shell and tube sides of the heat exchanger. The heat transfer coefficients are then evaluated for each section. The following assumptions are made for computing the overall heat transfer coefficient of the test fluids:

- The heat losses are considered to be negligible.
- The specific heat of water and all test fluids are considered to be 1 Btu/lbm °F.

Results and Discussion

Variation in the heat transfer coefficients are performed for borate crosslinked 35 lb/Mgal Guar test fluid at 150^{o}F and pH 10. The heat transfer coefficients are averaged values over the different lengths of coiled tubing. The heat transfer coefficient is found to lie between 70 and 85 Btu/(^{o}F hr ft^2) for the range of shear histories considered. This small variation in the heat transfer coefficients is due to the rheological changes that fluid undergoes at the different shear histories. Due to a higher temperature difference between hot and cold fluids at the inlet section, a higher heat transfer coefficient is observed. Also, the heat transfer coefficient is found to be independent of crosslinker flow rate between 300 and 450 ml/min. Figure 11 shows the variation of overall relative heat transfer coefficient for borate-crosslinked 35 lb/Mgal Guar at different pH values and temperature of 120°F. This graph suggests that the pH 9 fluid has a higher heat transfer coefficient at all the considered shearing lengths. Also, there is a larger change in heat transfer coefficient of the fluids up to 1000 feet of coiled tubing length. Increasing coiled tubing lengths up to 5000 feet does not seem to have a significant effect on the overall heat transfer coefficient. The results show that the heat transfer coefficient for pH 9 fluid is higher than pH 11 fluid for all shearing lengths at 150^{0}F. In addition, the study on water shows that heat transfer coefficient for linear and crosslinked gels are significantly lower than those of water.

Future Activities

Results Verification and Technology Transfer

The FFCF plans to verify its past research findings by comparing them to that of the industry. In addition, the FFCF is in the process of transferring the past research results to the industry and research institutes.

Future Research Focus

The FFCF is also planning to utilize the state-of-the-art facility to expand the current investigations to other innovative research areas such as:

- Proppant Transport
- Rheology of Fluid with Breakers
- Crosslinked Gel Rheology
- Crosslinked Slurry Rheology
- Foam Fluids
- Carbon dioxide (CO_2)/Sand Stimulations
- Coiled Tubing Applications
- Proppant Flowback

Conclusions

- An optimum crosslinked gel formulation characterized by a shear history independent and maximum viscosity is found to exist at a particular pH value for each temperature investigated between shear rates ranging from 20 to 200 sec^{-1}.
- New reliable correlations have been developed for perforation pressure loss to provide the coefficient of discharge for linear polymer solutions, titanium/borate-crosslinked gels, and linear slurries prepared with 20/40 mesh sand.
- The change in the coefficient of discharge due to perforation erosion is a complex function of sand size, sand concentration, perforation diameter, carrier fluid viscosity, flow rate, and pumping time.
- Surface roughness is a major factor in filter cake development.
- Filter cake development is not a requirement for fluid loss control.
- For linear fluids, fluid loss follows a linear with square-root-of-time relationship, while the fluid loss for crosslinked fluids shows a departure from this behavior with the time of departure depending on the permeability.
- Increasing the gel concentration enhances fluid loss control.
- The addition of silica flour enhances fluid loss control; however, increasing the concentration of silica flour provides no further enhancement.
- For water, the tubing seam decreases the frictional pressure loss whereas coiled tubing curvature increases the frictional pressure drop with magnitude of the effect of curvature being much greater than that of the seam.
- While the tubing seam does not seem to have any effect on frictional pressure loss for the

linear solutions, the curvature of the coiled tubing strongly affects the pressure drop.

- For borate-crosslinked gels, the frictional pressure loss is a strong function of pH and shear history.
- The overall heat transfer coefficient for borate-crosslinked 35 lb/Mgal Guar gel, ranges from 70 and 85 Btu/(^{o}F hr ft^{2}) for shear histories up to 3000 ft.
- Heat transfer coefficient for linear and crosslinked gels are lower than those of water.
- The overall heat transfer coefficients for the borate crosslinked Guar are independent of crosslinker flow rate between 300 and 450 ml/min.
- The overall heat transfer coefficients depend on crosslinker flow rates between 450 and 500 ml/min due to a higher degree of crosslinking.

Nomenclature

Fluid Rheology

H = height of the slot, ft
L = distance between pressure ports, ft
ΔP = pressure drop, psi
Q = volumetric flow rate, gpm
w = gap width of the slot, in.
τ_w = wall shear stress, psf
$\dot{g}$ = nominal shear rate, sec^{-1}
μ_a = apparent viscosity, cp

Perforation Pressure Loss

A = kinetic energy constant
B = kinetic energy exponent
C_d = perforation coefficient of discharge
d = initial perforation diameter, in.
N = number of perforations
ΔP = pressure drop, psi
Q = flow rate, gpm
r^2 = correlation coefficient
ρ = fluid density, lb/gal
Π = dimensionless group
μ_a = apparent viscosity, cp

Tubular Friction Loss

f_{SP} = straight pipe friction factor
f_{CT} = coiled tubing friction factor
N_{Re} = Newtonian Reynolds number

Heat Transfer

A = exposed area to heat transfer, ft^2
C_P = specific heat, Btu/lb ^{o}F
C_w = fluid loss coefficient, ft/min$^{1/2}$
Q_v = volumetric flow rate, gal/min
U = heat transfer coefficient, Btu/(^{o}F hr ft^{2})
ΔT = temperature difference, ^{o}F
ΔT_L = log. mean temperature difference, ^{o}F
$\Delta T_1 = T_{ho} - T_{ci}$, ^{o}F
$\Delta T_2 = T_{hi} - T_{co,}$ ^{o}F
ρ = fluid density, lb/gal

References

1. Dawson, J. C.:"A Thermodynamic Study of Borate Complexation with Guar and Guar Derivatives," paper SPE 22837 presented at the 1991 SPE Annual Conference and Exhibition, Dallas, Oct. 6-9.
2. Harris, P. C.:"Chemistry and Rheology of Borate-Crosslinked Fluids at Temperatures to 300°F," *JPT* (Mar. 1993) 264-269.

3. Prud'homme, R. K.:"Rheology of Fracturing Fluid Slurries," GRI Topical Report, Contract 5089-211-1880, (Sept. 1996).
4. Lagrone, K., and Rasmussen, J.:"A New Development in Completion Methods-The Limited Entry Technique", *JPT*, July 1963, 693-702.
5. Lord, D. L., Shah, S. N., Rein, R. G. Jr., and Lawson, J. T. III:"Study of Perforation Friction Pressure Employing a Large-Scale Fracturing Flow Simulator," paper SPE 28508 presented at the 1994 Annual Technical Conference, New Orleans, Louisiana, September 25-28.
6. Penny, Glenn S. and Conway, Michael W.: *Recent Advances in Hydraulic Fracturing*, pp. 147-176, SPE 1992
7. Hall, C.D., Jr. and Dollarhide, F.E.: "Effects of Fracturing Fluid Velocity on Fluid-Loss Agent Performance," Trans., AIME (1964) 231, 555-560.

Acknowledgments

The authors wish to thank Gas Research Institute, the U.S. Department of Energy, and the University of Oklahoma for Funding this project and permission to publish this work. MTS Systems Corporation designed, built, and installed the apparatus and has participated in the project since its inception. Halliburton Energy Services has also participated in the project and has supplied auxiliary equipment.

Figure 1- The High Pressure Simulator at the FFCF

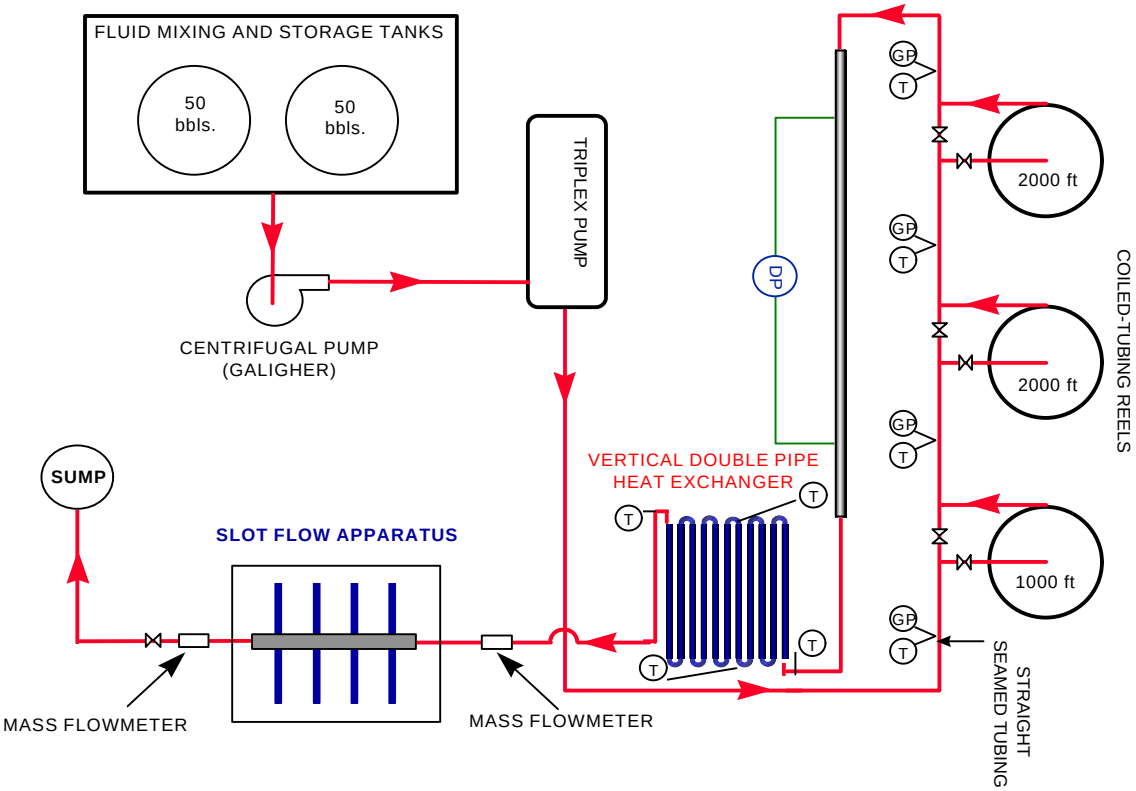

Figure 2- The Auxiliary Equipment Layout at the FFCF

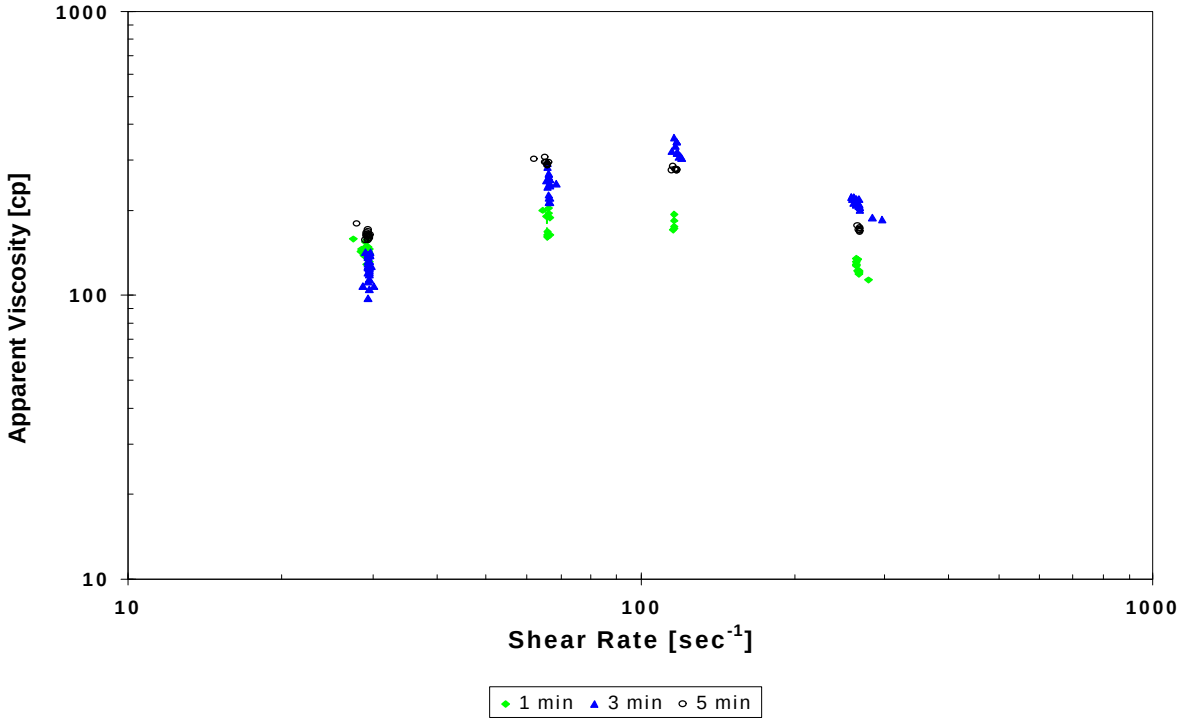

Figure 3- Variation of Apparent Viscosity with Shear Rate for pH 9 Borate-Crosslinked 35 lb/Mgal Guar Gel at 150°F for Various Shear Durations at 1400/s

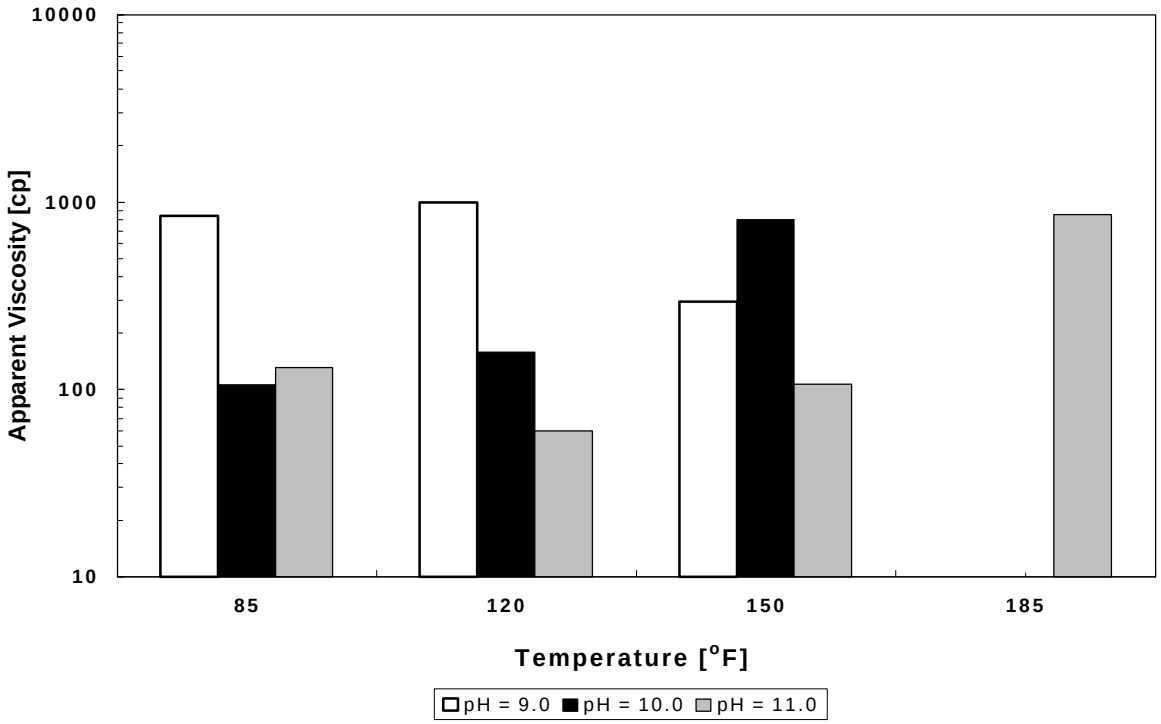

Figure 4- Apparent Viscosity at Various pH and Temperatures for Borate-Crosslinked 35 lb/Mgal Guar Gel at a Shear Rate 65/s and Shear History of 5 min at 1400/s

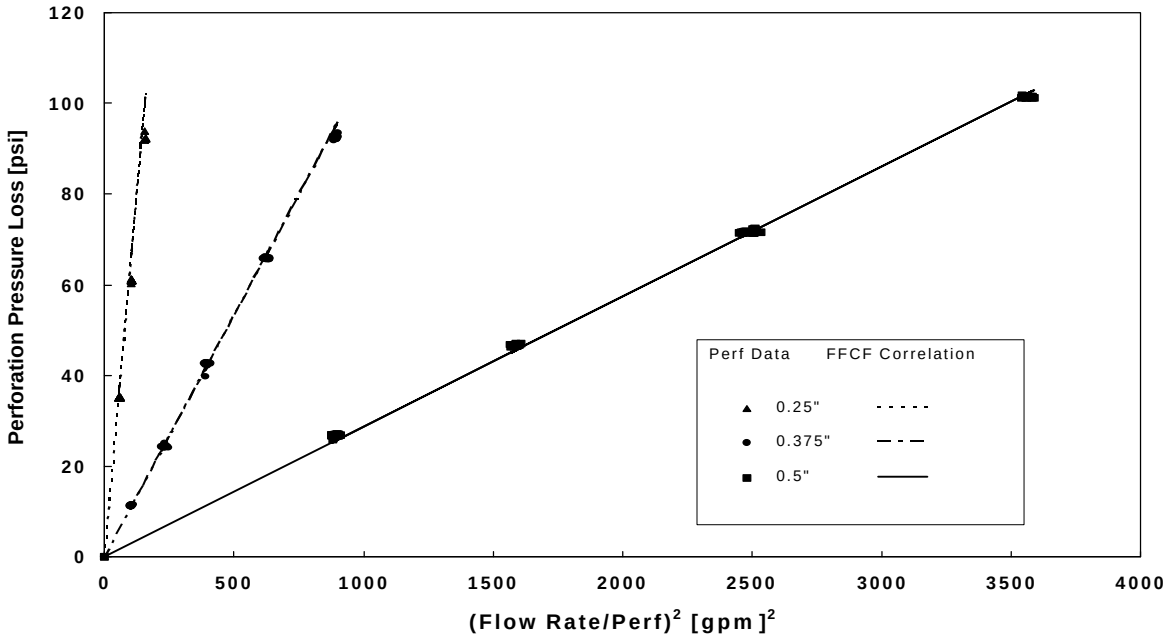

Figure 5-Correlation Predictions of ΔP for 35 lb/Mgal Guar

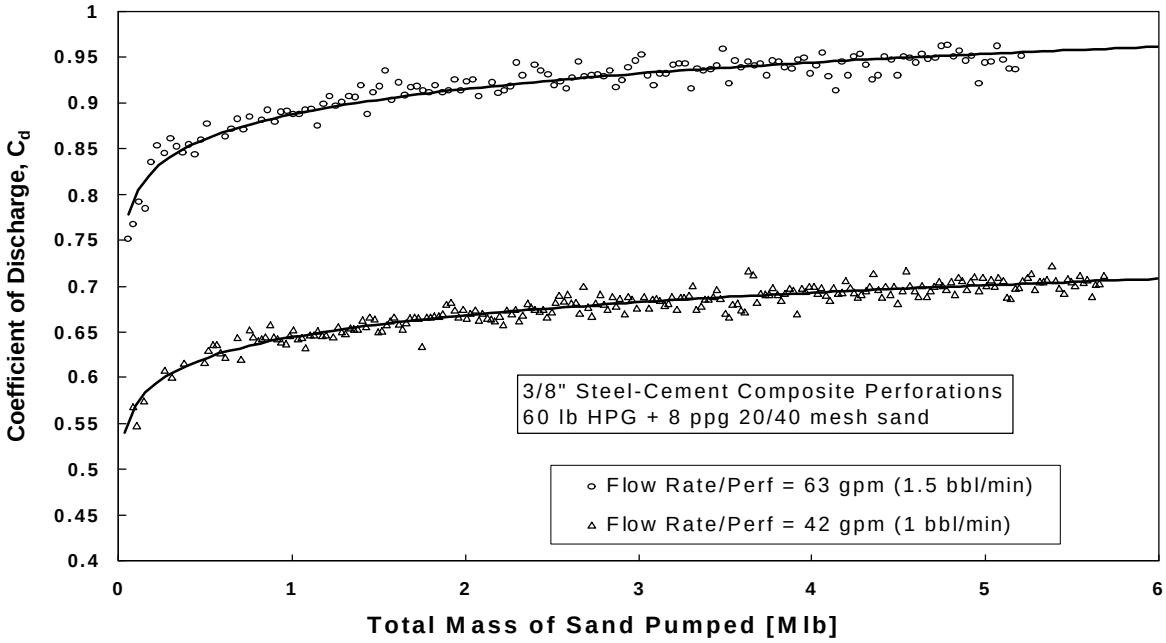

Figure 6-Coefficient of Discharge as a Function of Total Cumulative Mass of Sand Pumped; 60 lb HPG+20/40 Mesh Sand

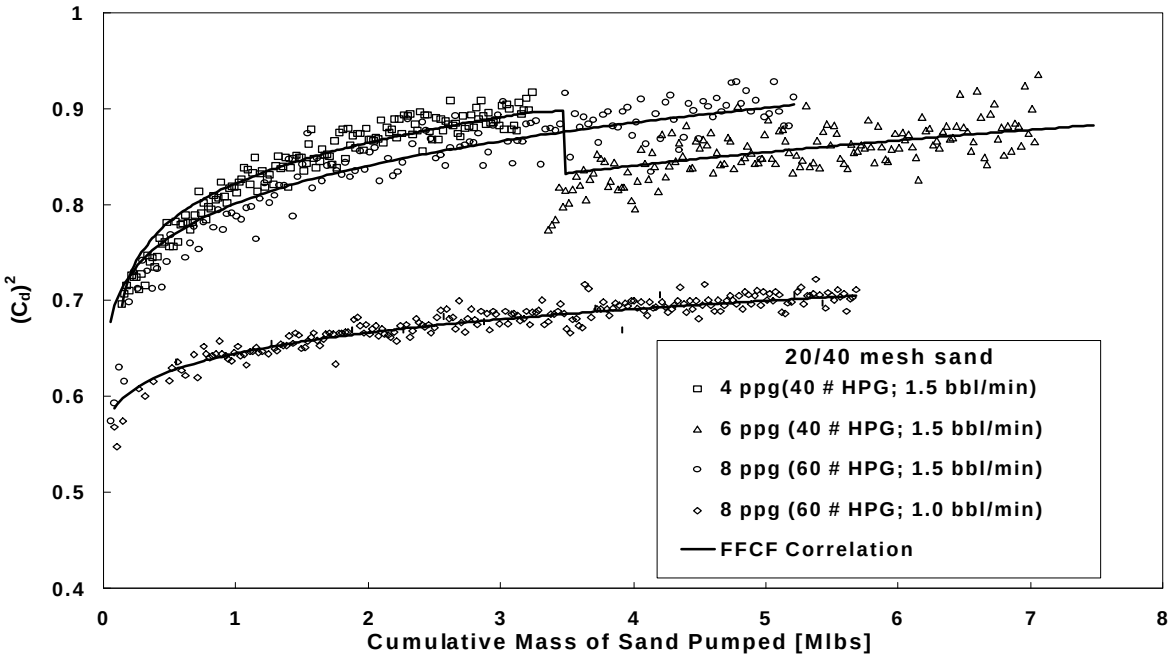

Figure 7- Empirical Model Fit of Experimental Data

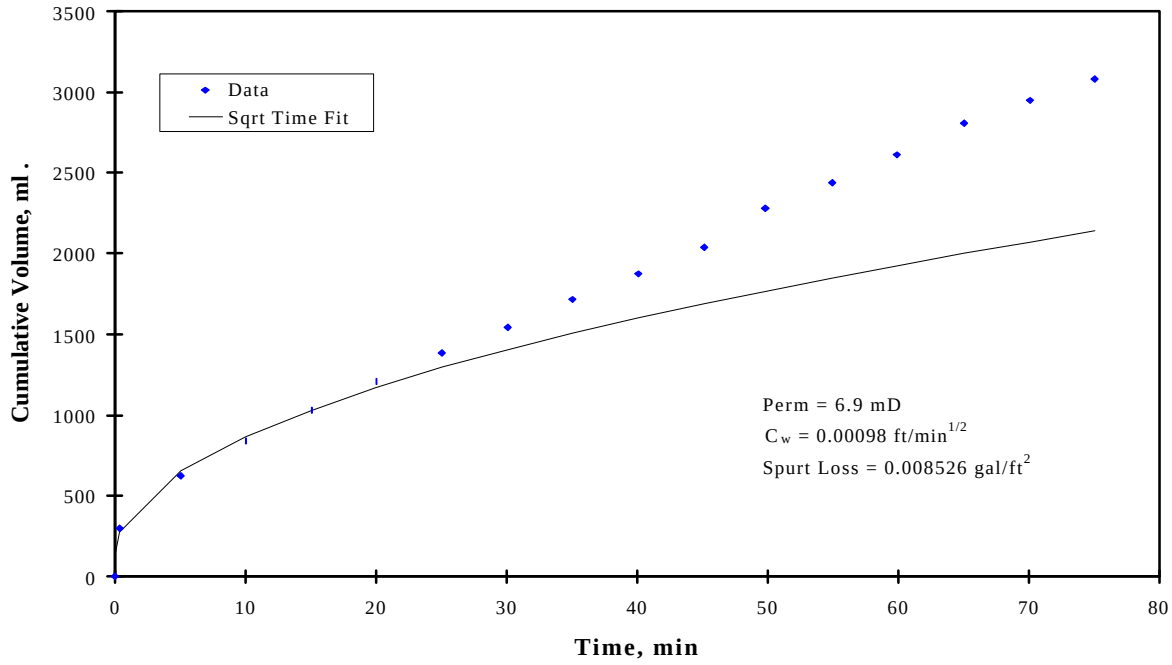

Figure 8- Borate Crosslinked 35 lb/Mgal HPG without Silica Flour on Synthetic Rock

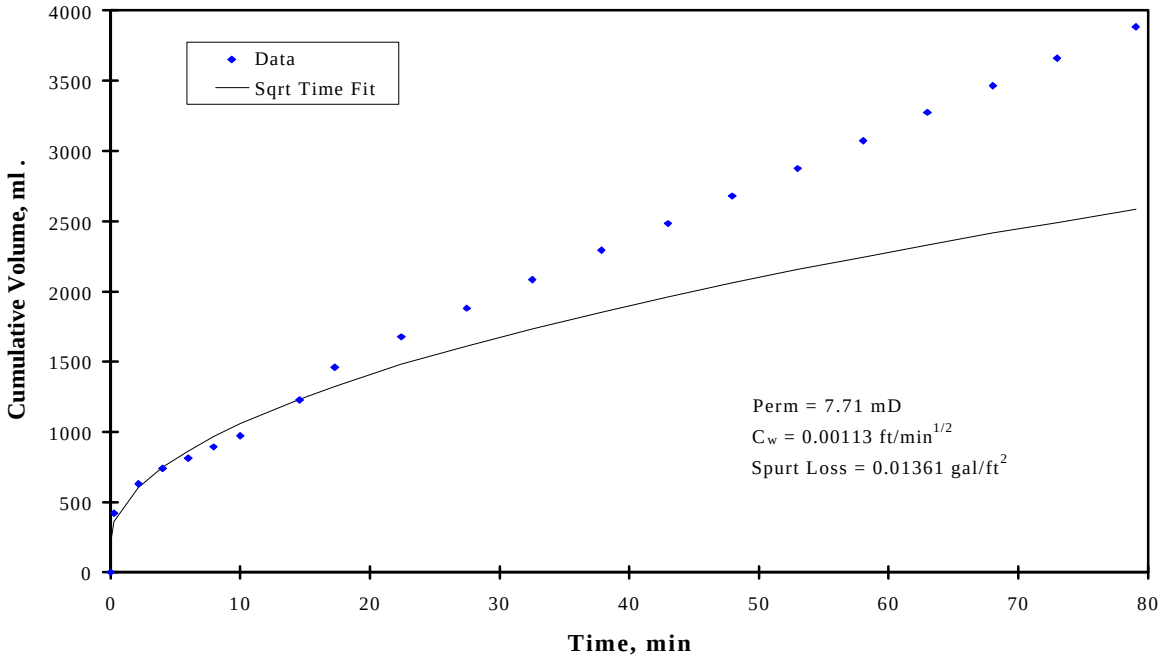

Figure 9- Borate Crosslinked 35 lb/Mgal HPG with 25 lb/Mgal Silica Flour on Synthetic Rock

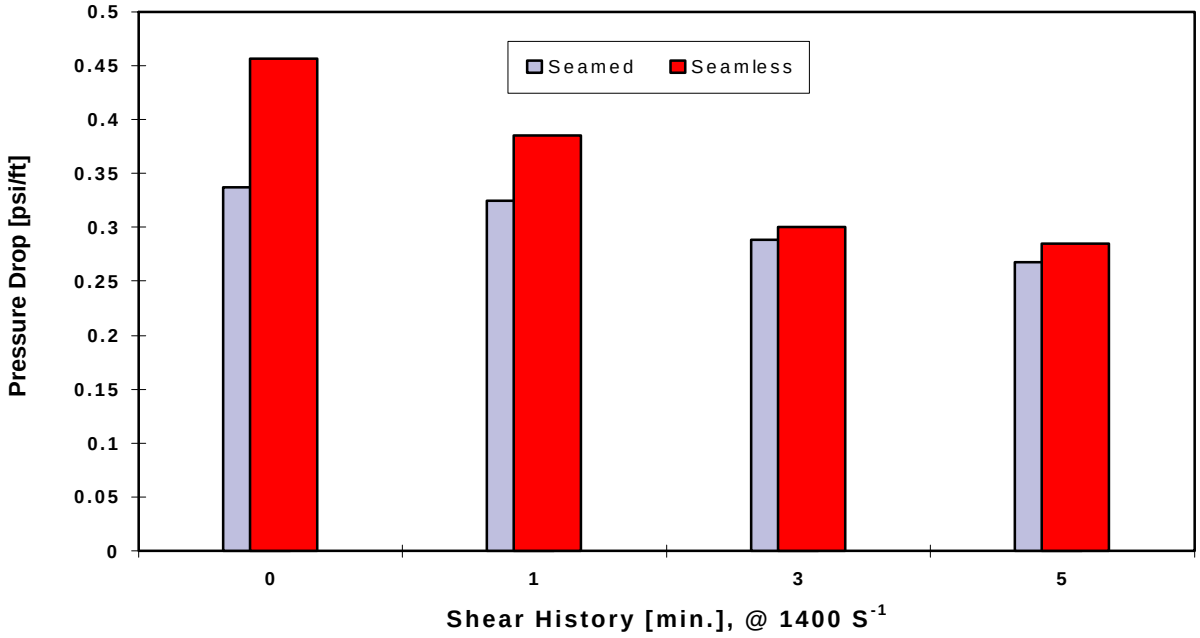

Figure 10- Pressure Drop in Seamed and Seamless Tubing for pH 9 Borate-Crosslinked 35 lb Guar/Mgal Gel, Flow Rate of 60 gpm

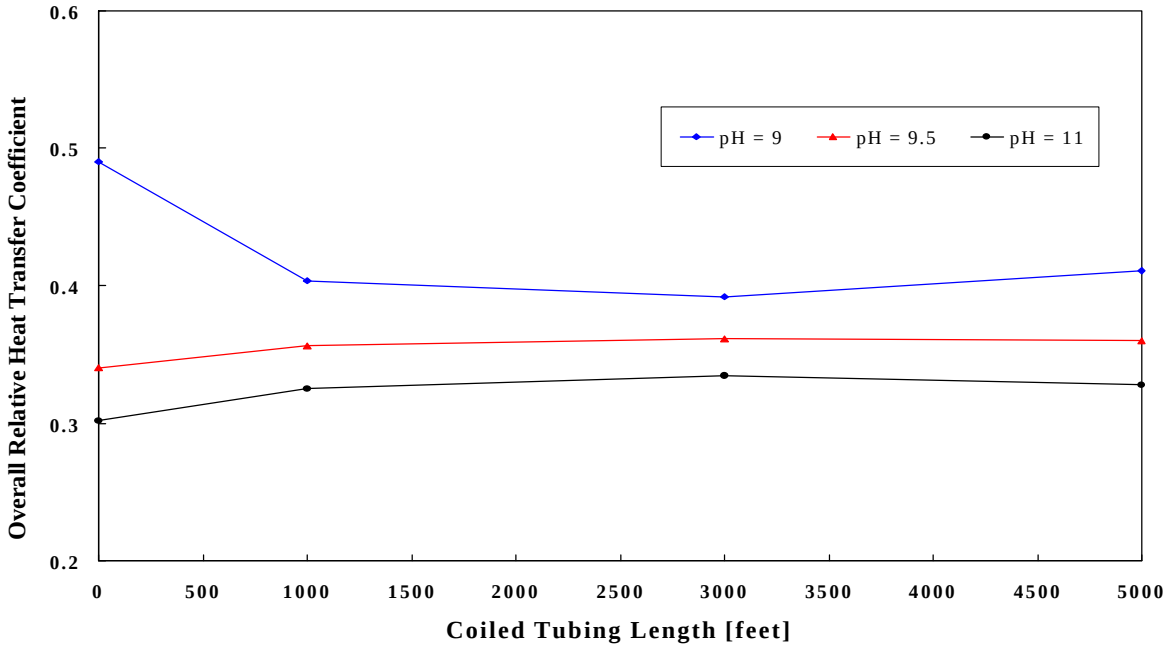

Figure 11- Borate Crosslinked 35 lb/Mgal Guar at 120°F and a Flow Rate of 60 gpm